Multiplex Sensing of Protease and Kinase Enzyme Activity *via* Orthogonal Coupling of Quantum Dot–Peptide Conjugates

Stuart B. Lowe,[†,‡] John A. G. Dick,[†,‡] Bruce E. Cohen,[⊥] and Molly M. Stevens[†,‡,§,*]

[†]Department of Materials, [‡]Institute of Biomedical Engineering, and [§]Department of Bioengineering, Imperial College London, Exhibition Road, London SW7 2AZ, U.K. and, [⊥]Biological Nanostructures Facility, The Molecular Foundry, Lawrence Berkeley National Laboratory, Berkeley, California 94720, United States

ABSTRACT Nanoparticle-based labels are emerging as simpler and more sensitive alternatives to traditional fluorescent small molecules and radioactive reporters in biomarker assays. The determination of biomarker levels is a recommended clinical practice for the assessment of many diseases, and detection of multiple analytes in a single assay, known as multiplexing, can increase predictive accuracy. While multiplexed detection can also simplify assay procedures and reduce systematic variability, combining multiple assays into a single procedure can lead to complications such as substrate cross-reactivity, signal overlap, and loss of sensitivity. By combining the specificity of biomolecular interactions with the tunability of quantum dot optical properties, we have developed a detection system capable of simultaneous evaluation of the activity of two critical enzyme classes, proteases and kinases. We avoid cross-reactivity and signal overlap by synthesizing enzyme-specific peptide sequences with orthogonal terminal functionalization for attachment to quantum dots with distinct emission spectra. Enzyme activity is reported *via* binding of either gold nanoparticle–peptide conjugates or FRET acceptor dye-labeled antibodies, which mediate changes in quantum dot emission spectra. To the best of our knowledge, this is the first demonstration of the multiplexed sensing of the activity of two different classes of enzymes *via* a nanoparticle-based activity assay. Using the quantum dot-based assay described herein, we were able to detect the protease activity of urokinase-type plasminogen activator at concentrations ≥ 50 ng/mL and the kinase activity of human epidermal growth factor receptor 2 at concentrations ≥ 7.5 nM, levels that are clinically relevant for determination of breast cancer prognosis. The modular nature of this assay design allows for the detection of different classes of enzymes simultaneously and represents a generic platform for high-throughput enzyme screening in rapid disease diagnosis and drug discovery.

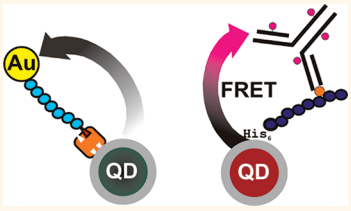

KEYWORDS: quantum dots · multiplexing · FRET · biosensors · bionanotechnology · enzyme activity · breast cancer

Biofunctionalized nanoparticles (NPs) are emerging as an alternative class of molecular reporter in biomarker assays,[1−5] with demonstrable advantages in simplicity[6] and sensitivity[7] over the more traditional fluorescent small molecules and radioactive labels. In this article, we describe a detection system capable of simultaneous evaluation of the enzymatic activity of urokinase-type plasminogen activator (uPA), a serine protease, and human epidermal growth factor receptor 2 (Her2), a receptor tyrosine kinase. Breast cancer is the most commonly occurring cancer in women, and survival rates vary greatly depending on time of detection (and thus disease progression), chance of metastasis, and cancer phenotype. An accurate prognosis can guide treatment strategy and hence is a crucial parameter for both physician and patient. Determination of biomarker levels is a recommended clinical practice for assessing breast cancers.[8] uPA has been implicated in cancer invasion and metastasis, both through direct degradation of the extracellular matrix (ECM) and by increased activation of its substrate, plasmin, which is a particularly destructive ECM-degrading protease.[9,10] Her2 is a receptor tyrosine kinase and has been found to be overexpressed in over 20% of breast cancers.[11] High levels of Her2 can indicate resistance to certain modes of treatment and a generally poorer prognosis.[12] The major consequence of Her2 overexpression in cancers is promotion of signaling pathways leading to increased invasion propensity.[13−15] The biomarker pair of uPA protease and Her2 kinase has been shown to provide significant prognostic information in terms of the metastasis-free survival of breast cancer patients[16] and, hence, represents a promising system for proof-of-concept demonstration of our proposed multiplexed approach. Given that many diseases can be characterized by aberrant action of enzymes, we propose to detect the biomarker pair by virtue of their enzymatic activity. The clinical cutoffs for negative/positive prognosis as determined by Konecny *et al.*[16] are 5.5 ng/mg protein for uPA and 400 fmol/mg protein for Her2, in pulverized biopsy samples. This translates to a desired assay sensitivity of 200 ng/mL for uPA and 15 nM for Her2.[17]

Quantum dots (QDs) are semiconductor nanocrystals with size-dependent optical

* Address correspondence to m.stevens@imperial.ac.uk.

Received for review November 10, 2011 and accepted December 13, 2011.

Published online December 13, 2011
10.1021/nn204361s

properties. QDs possess strong resistance to photobleaching, narrow and intense emission spectra, and a wide excitation spectrum in the UV range, allowing for QDs with separate emissions to be excited with a common source. In the assay reported here, the QDs act simultaneously as both reporter and scaffold for synthetic substrate peptides, and the nanoscale dimensions of the QDs increase the ensemble surface area available for sensing. Systems capable of detecting multiple targets are of particular interest for a number of applications, including high-throughput drug screening and rapid, point-of-care diagnostics. Improvements in assay reproducibility could be realized due to the ability to include internal controls and because of a reduction in sampling errors.[18]

Activity-dependent Förster resonance energy transfer (FRET)-based QD-peptide sensors have been used to detect cleavage events resulting from caspase-1, thrombin, chymotrypsin,[19] and collagenase[19,20] proteolysis. Kim *et al.*[21] previously employed a QD-gold nanoparticle (AuNP)-based system for the detection of MMP-7, caspase-3, and thrombin proteases. In that study, AuNP-labeled peptide substrates were bound to QDs *via* streptavidin–biotin coupling, quenching the photoluminescence (PL) of the QDs. The PL was recovered *via* protease-mediated cleavage of the peptide and dissociation of the AuNPs. Chang *et al.*[22] used a similar architecture to detect collagenase; here, the peptides were covalently coupled to the QD surface. We previously developed highly sensitive assays for Src and Abl kinases[23] and p300 acetyltransferase[6] activity determination, and a similar architecture was employed by Freeman *et al.*[24] Enzyme-specific substrate peptides were immobilized on the QD surface, and an activity-based signal was developed *via* the introduction of dye-labeled antibodies, which resulted in FRET. QDs have been incorporated into antibody–antigen recognition platforms for the multiplexed detection of biomarkers.[18,25] In general, to achieve multiplexed detection utilizing QDs, a number of conditions must be met, including specific recognition of analytes and simultaneous resolution of positive and negative signals from different analytes.

Here, we have designed a multicomponent, solution-based assay with sensitivity to both protease and kinase activities. Enzyme specificity was realized by synthesizing peptides with amino acid recognition sequences based on enzyme–substrate interaction studies.[26,27] Activity determination is reliant on self-assembly of the peptides to specific motifs on the QD surface. Signal independence for each target was achieved by using two QD populations with different emission wavelengths and orthogonal surface functionalizations. In contrast with other QD-based activity assays,[21,28] our system is able to multiplex more than one family of enzymes. The developed multiplex assay is a homogeneous, three-stage procedure, illustrated in Scheme 1. The first stage is an incubation of the mixed enzyme sample with the substrate peptides. Each peptide is specific against either uPA protease or Her2 kinase. Considering each peptide in turn, the uPA substrate (blue) has the following architecture: (i) N-terminal biotin for coupling to the streptavidin-labeled QD; (ii) uPA recognition sequence Ser-Gly-Arg↓Ser-Ala-Asn derived from phage display studies[26] (arrow indicates cleavage point); (iii) C-terminal cysteine residue covalently coupled to a monomaleimide-functionalized, 1.4 nm diameter AuNP, for quenching of the QD PL. The Her2 target peptide (purple) has the following structure: (i) N-terminal His tag composed of six consecutive histidine residues, with strong affinity for the ZnS shell of the 3-mercaptopropionic acid (MPA)-capped QD;[29] (ii) spacer (Gly-Gly-Gly) to improve antibody accessibility of peptides when they self-assemble onto the QD surface; (iii) C-terminal Her2 recognition sequence Asp-Asn-Glu-Tyr*-Phe-Tyr-Val, based on kinase-activity assays from Kerman[27] and others (starred residue is preferentially phosphorylated). During the enzyme incubation, the uPA substrate peptides are susceptible to hydrolytic cleavage, and the Her2 substrate peptides can be phosphorylated at the target tyrosine residue. We expect the degree of cleavage (due to uPA) and/or phosphorylation (due to Her2) to be dependent on the respective enzyme activities.

Following the enzyme–substrate incubation, the next stages of the assay are intended to provide an activity-dependent readout for the assay. The second stage is the self-assembly of substrate peptides onto the surface of QDs. We use streptavidin-coated QDs with a nominal emission maximum at 525 nm (QD525) and MPA-coated QDs with a nominal emission maximum at 655 nm (QD655). In order to detect both enzymes in the same sample simultaneously, it was important to use an orthogonal coupling strategy. The system is designed so that during the peptide–QD self-assembly the biotinylated uPA substrate specifically binds to the streptavidin present on the QD525 surface, and the His-tagged Her2 substrate binds to the surface of the QD655 by metal-affinity coordination. The effect of this is to generate two populations of peptide–QD conjugates, which will each produce an independent enzyme-specific signal. In the third stage, an AlexaFluor 660 (AF660) dye-labeled anti-phosphotyrosine antibody is introduced, which can form an immunocomplex in the presence of phosphorylated tyrosine residues and induce a FRET coupling between the AF660 dyes and the proximal QD655. In justifying this particular assay design, we wished to create a generic multiplex platform and, thus, took into account a number of general considerations about the substrates and method of QD quenching. In order to detect proteolysis, which involves the cleavage of a peptide bond, it was desirable to physically link the QDs with the quencher molecule *via* the peptide of interest. AuNPs were selected to transduce the protease-related signal because of their particularly strong QD quenching ability

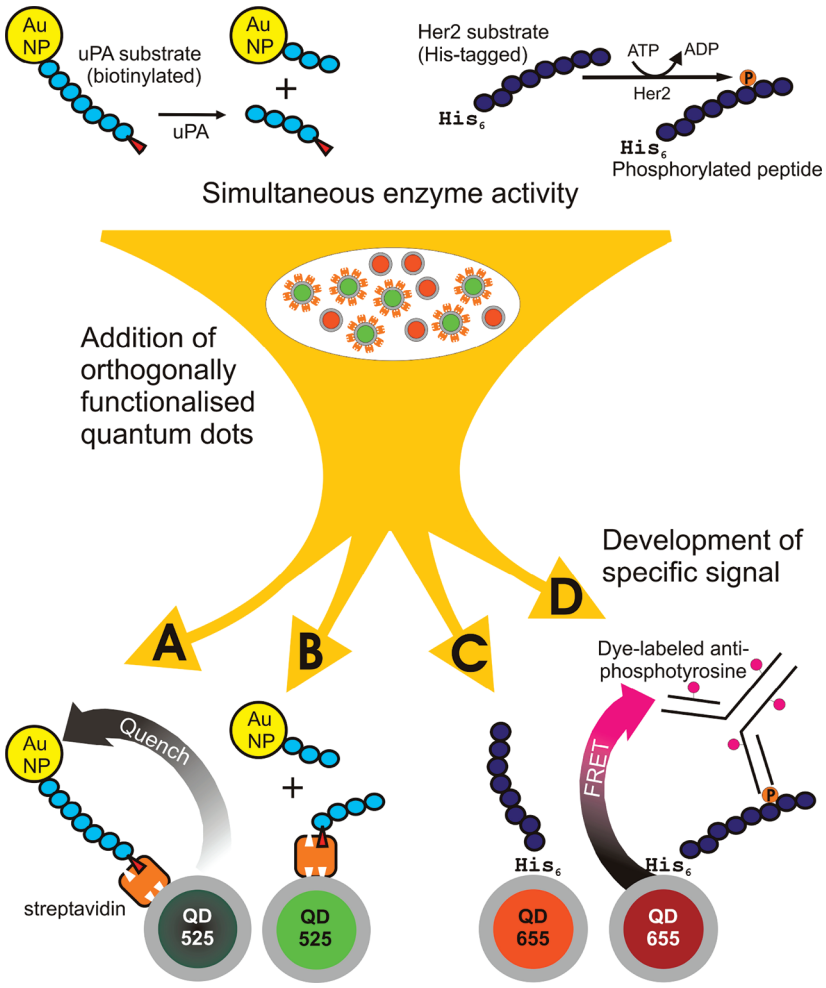

Scheme 1. Multiplexed detection of uPA protease and Her2 kinase. Peptide substrates are simultaneously incubated with uPA and Her2 enzymes. uPA mediates proteolytic cleavage of AuNP-labeled uPA substrate peptide (blue), while Her2 mediates phosphorylation of Her2 substrate peptide (purple). Following enzyme incubation, a mixture of streptavidin-coated QD525s and MPA-coated QD655s is added, resulting in self-assembly of the configurations A–D (only one peptide per quantum dot shown for clarity). (A) Uncleaved uPA substrates form a QD525-peptide-AuNP complex *via* biotin–streptavidin interaction, and QD525 emission is quenched. (B) Cleavage of uPA substrate prevents AuNP binding, and QD525 emission remains unquenched. (C and D) His-tagged Her2 substrates bind to QD655 *via* metal-affinity coordination; however only when the substrate peptides are phosphorylated (D) does the introduction of AF660-labeled anti-phosphotyrosine lead to immunocomplex formation and Förster resonant energy transfer (FRET).

with no re-emission;[30] for the kinase (or more generally, transferase) detection, where a functional group is appended to the peptide, we decided to detect the specific modification by means of immunorecognition by an antibody. In this case, the kinase-dependent signal would be caused by labeling the antibody with a FRET acceptor. This approach allows for the flexibility of coding for different enzyme targets using differently colored dye labels. In Scheme 1, the conjugate configurations A–D that would give rise to negative and positive enzyme signals are shown. Configuration A will arise when there is no uPA present. Configuration B will occur at high uPA concentrations. Configuration C represents the situation in the absence of Her2, and configuration D represents the condition of high Her2 concentration. At intermediate uPA and Her2 concentrations, most QDs will display a hybrid configuration due to QD polyvalency; some of the peptides will be modified, and some will not. The QD polyvalency will allow the assay to display a continuous range of sensitivity, rather than discrete steps.

We prepared control samples to verify the orthogonal coupling strategy. The QD525 controls (configurations A and B, Scheme 1) were mixed with the QD655 controls (configurations C and D, Scheme 1), giving rise to four possible permutations (for more information on control samples, see the Methods section). PL spectra of the resulting QD bioconjugates are shown in Figure 1. The binding of labeled uPA substrates (QD525 A) resulted in a decrease in the PL at 520 nm (red/blue lines) due to a quenching of the QD525 PL by proximal AuNPs. In the case of unlabeled uPA substrates (QD525 B), the AuNP did not interact with the QD525 surface; hence the PL at 520 nm was higher (black/green lines). In samples containing phosphorylated Her2 substrate

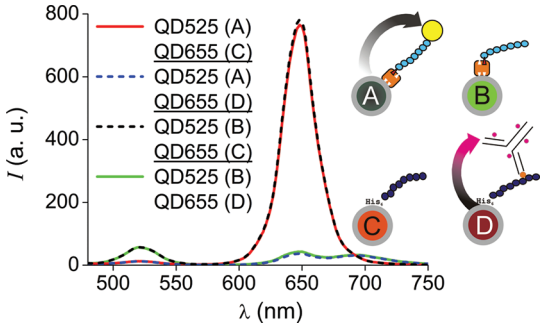

Figure 1. PL spectra of mixtures containing bioconjugated QD525 (final concentration 10 nM) and QD655 (final concentration 50 nM). QD525 decorated with Au NP-labeled (A) or unlabeled (B) uPA substrate peptides. QD655 decorated with unmodified (C) or phosphotyrosine-substituted (D) Her2 substrate peptides and incubated with AlexaFluor660 dye-labeled anti-phosphotyrosine antibodies.

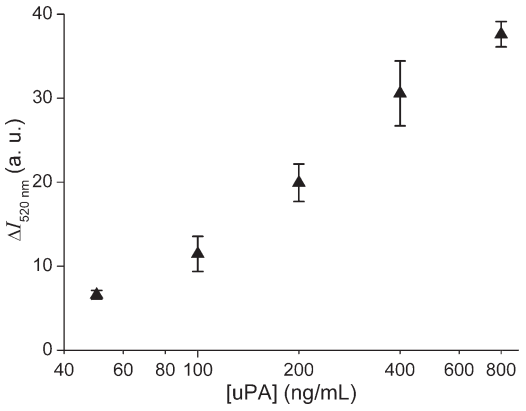

Figure 2. Quantification of uPA activity by monitoring PL peak of QD525 functionalized with uPA substrate peptides labeled with 1.4 nm AuNPs. Change in PL from basal level (no uPA added) is plotted after incubation with varying concentrations of uPA.

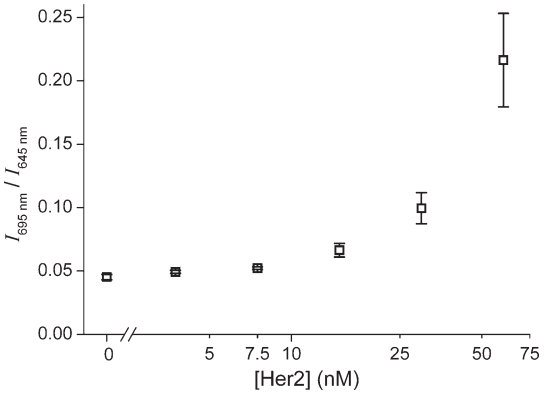

Figure 3. Quantification of Her2 activity by monitoring ratio of PL intensities at 695 nm (dye peak) and 645 nm (QD peak). Her2 substrate peptides incubated with varying concentrations of Her2 kinase in the presence of ATP. Signal developed by incubating peptides with QD655 and AF660 dye-labeled anti-phosphotyrosine antibodies.

peptide (QD655 D), the assembly of a QD655-phosphopeptide-antibody immunocomplex resulted in a decrease in the PL at 645 nm accompanied by an increase in emission at 695 nm (blue/green lines). This behavior is characteristic of FRET coupling between the QD655 emission and the AF660 dyes with overlapping absorption spectra due to proximal binding of the dye-labeled antibody (Förster radius of FRET pair = 60 Å; see SI for calculation). The FRET response is consistent with that observed by Nikiforov *et al.*[31] In the case of unphosphorylated peptides (QD655 C), there is no immunorecognition, and there is a large QD655 emission peak at 645 nm (red/black lines). The QD655 FRET response is quantified by taking the ratio between the dye emission and the QD655 emission ($I_{695\ nm}/I_{645\ nm}$). The spectral changes due to uPA substrate self-assembly and Her2 substrate immunocomplex formation are independent of each other and indicate that the orthogonal coupling approach is robust to cross-reactivity and nonspecific binding.

Enzyme titrations were performed individually for uPA (Figure 2) and Her2 (Figure 3) to determine the ultimate limit of detection and demonstrate that the assays are activity-based. Using AuNP-labeled uPA substrate peptides, it was possible to detect uPA *via* its proteolytic activity. In the blank containing no uPA, the QD525 PL was quenched because all of the substrate peptides remained uncleaved. As the concentration of uPA was increased above 50 ng/mL, peptide cleavage was observed by monitoring the increase in PL above the blank. In Figure 2, the PL was observed to increase with increasing uPA concentration. By contrast, control samples omitting AuNPs (Supporting Information, Figure S1, white data points) showed negligible increase in PL. These data indicate that the system is sensitive to the proteolytic activity of uPA and not just total protein concentration. The measured limit of detection was 50 ng/mL uPA.

In the case of Her2, the development of an activity-dependent signal was based on FRET between QD655 and AF660. In the presence of the cofactor, ATP, the concentration of Her2 determines the degree of substrate phosphorylation. In Figure 3, the ratio of AF660 dye emission to QD655 emission ($I_{695\ nm}/I_{645\ nm}$) was observed to increase with increasing Her2 concentration. This was due to the binding of multiple AF660-labeled anti-phosphotyrosine antibodies to the QD655, inducing FRET. By contrast, in the absence of Her2 or ATP (Supporting Information, Figures S2 and S3, white triangular data points) the immunocomplex was not formed, and the $I_{695\ nm}/I_{645\ nm}$ ratio remained at a basal level of 0.045 (corresponding to no FRET). Removal of ATP eliminated FRET, which indicates that the assay is activity dependent. The measured limit of detection was 7.5 nM Her2.

In terms of the clinical significance of this assay, the measured limit of detection for uPA is 50 ng/mL, and for Her2 it is 7.5 nM, both of which are below the negative/positive cutoffs set by Konecny *et al.*[16] Samples containing mixtures of the two enzymes were probed experimentally,

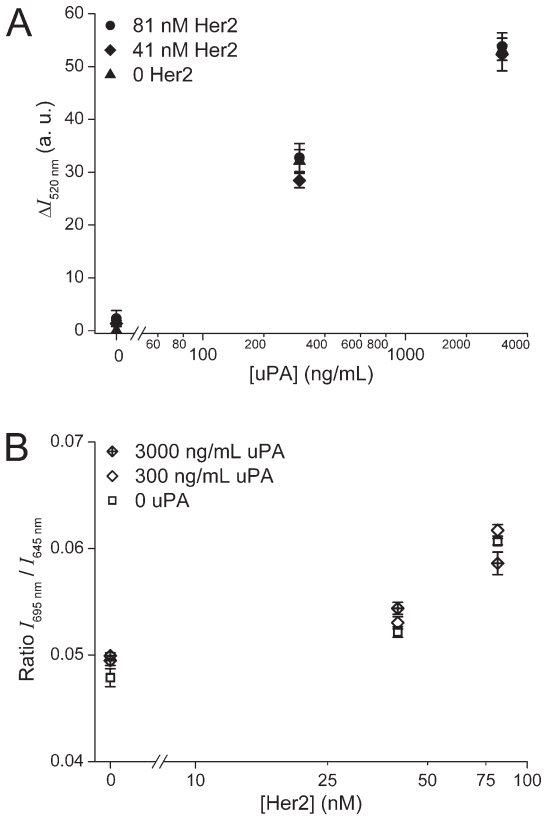

Figure 4. Simultaneous detection of uPA and Her2 in the multiplexed format. (A) Change in PL at 520 nm plotted against uPA concentration for samples containing varying amounts of uPA and Her2 (Her2 concentrations denoted by differently shaped data points). (B) $I_{695\ nm}/I_{645\ nm}$ ratio plotted against Her2 concentration in sample. (uPA concentrations denoted by differently shaped data points.)

and signal independence was demonstrated by testing a range of conditions at differing enzyme concentrations. In Figure 4A, the trend for PL increase with increasing uPA concentration, irrespective of Her2 concentration, can be observed. In Figure 4B, the trend for $I_{695\ nm}/I_{645\ nm}$ to increase with increasing Her2 concentration, irrespective of uPA concentration, can be observed. It was possible to distinguish between the groups of data at different enzyme concentrations with >95% confidence. Hence, we demonstrated that there was no cross-reactivity, either between the enzymes and the substrates or between the peptides and the QDs. The assay was enzyme-specific, and the signals were well-resolved.

This QD-based multiplexed assay represents a simple, sensitive method for enzyme activity determination. The method is solution-based and does not require washing steps or disposal of radioactive materials. The limit of detection for uPA protease is 50 ng/mL, which improves on the limit of 500 ng/mL uPA determined by BRET (bioluminescence resonance energy transfer).[28] The limit of detection of Her2 kinase is measured to be 7.5 nM, which corresponds to low mU/μL activity levels in accordance with the limits of detection for Src and Abl kinases published previously.[23] The high sensitivity of our QD-FRET assay is achieved due to the large ensemble surface area and multiple ligand binding sites per QD (~30 binding sites per QD525[21] and up to 140 binding sites per QD655[32]). The dynamic range of the assay could be modulated by altering the ratio of peptides:QDs used or by changing the enzyme incubation time. Simultaneous readout of signals from the same sample reduces the effect of well-to-well variation. Detection of uPA and Her2 activity at clinically relevant levels[16] can provide physicians with prognostic information for breast cancer patients. In terms of applicability of this system for assaying clinical samples, particularly with regard to the stability of MPA-capped QDs, there is some evidence to suggest that His-tagged peptides can penetrate the PEG layer of PEG-passivated QDs,[33] which could offer a strategy for improving the stability of QDs in biological media while still preserving the biosensing properties. The specificity of both the biotin–streptavidin interaction[34] and the His tag-metal affinity interaction[35] has been demonstrated in complex biological media. Hence, there is a promising potential to modify this system for the detection of enzymes in clinically derived samples. To the best of our knowledge, this is the first demonstration of the multiplexed sensing of two different classes of enzymes *via* a NP-based enzyme activity assay. This system is generic in nature, and we have previously optimized the constituent components for a range of enzymes, *i.e.*, proteases (unpublished data), kinases,[23] and acetyltransferases;[6] hence this assay has exciting potential applications as a platform for high-throughput drug discovery and complements existing nanoparticle-based assays for cancer biomarkers.

MATERIALS AND METHODS

Quantum Dots. Qdot 525 ITK streptavidin conjugates (QD525) and Qdot 655 ITK organic quantum dots (QD655) were purchased from Invitrogen. The QD655 were rendered hydrophilic by ligand exchange with 3-mercaptopropionic acid (MPA) into borate buffer using the protocol of Pong *et al.*[36]

Peptides. uPA substrate peptide (biotin-SGRSANC-$CONH_2$) and Her2 control peptide (HHHHHHGGGDNE(pY)FYV-$CONH_2$) were purchased from LifeTein. Her2 substrate peptide (HHHHHHGG-GDNEYFYV-$CONH_2$) was synthesized by standard automated Fmoc solid-phase peptide synthesis from a Rink-amide solid support on a PTI Quartet peptide synthesizer. The peptides were cleaved and deprotected with 92.5:5:2.5 trifluoroacetic acid (TFA)/triisopropylsilane/H_2O for 3 h and precipitated and washed with cold diethyl ether. The crude peptides were purified to >90% (determined by MALDI) on a semipreparative C_{18} HPLC column using a water/acetonitrile mobile phase containing 0.1% (v/v) TFA.

Gold–Peptide Labeling. Monomaleimido Nanogold (1.4 nm gold NPs with single maleimide group) was purchased from Nanoprobes. The uPA substrate peptide (in 5 mM tris(2-carboxyethyl) phosphine solution) and Nanogold (in 10% v/v 2-propanol) were

mixed at a molar ratio of 10:1 in 25 mM HEPES (pH 7.5) for 24 h at 4 °C. Unlabeled peptide was removed by spin dialysis. The concentration of gold was calculated according to the manufacturer's instructions, and the conjugate was stored at 4 °C until use.

Antibody Labeling. Monoclonal anti-phosphotyrosine (Sigma, clone PT-66) was incubated with a 10-fold molar excess of AlexaFluor 660 succinimidyl ester (Invitrogen) in dimethylformamide (final DMF concentration <1%) for 1 h. The antibody was purified from excess dye *via* a Zeba Spin desalting column (Pierce). The ratio of dye/protein was calculated according to the manufacturer's instructions, and the conjugate was stored protected from light at 4 °C until use.

Enzymes. uPA was purchased from Calbiochem, and Her2 was purchased from Stratech Scientific. Before use, the Her2 enzyme was desalted to remove dithiothreitol, which affects the PL of the QDs.

Enzyme Reactions and Photoluminescence. Enzyme reactions were carried out in polypropylene microtubes. The reaction mixtures consisted of 1.1 μL of uPA, 4.1 μL of Her2, 3.0 μL of gold-labeled uPA substrate peptide (3.7 μM final concentration), 2.0 μL of Her2 substrate peptide (17 μM final concentration), and 1.5 μL of ATP (0.64 mM final concentration) in 25 mM HEPES (pH 7.5), 10 mM $MgCl_2$, and 0.01% w/v bovine serum albumin (BSA). The reactions were carried out for 3 h at 38.5 °C. MPA-capped QD655s were transferred to 25 mM HEPES (pH 7.5), 10 mM $MgCl_2$, and 0.01% w/v BSA by three repeated concentration/dilution cycles of centrifugal spin dialysis. Streptavidin-coated QD525 was diluted in the same buffer to a final concentration of 100 nM. The inclusion of BSA to a final concentration of 0.01% w/v provided enhanced colloidal stability and was necessary to avoid nonspecific binding. An aliquot of 7.8 μL of the peptide−enzyme reaction was added to a solution of QD525 (2.85 μL of 100 nM stock) and QD655 (13.32 μL of 100 nM stock), giving a uPA substrate peptide/QD525 ratio of 100:1 and a Her2 substrate peptide/QD655 ratio of 100:1. The mixture was vortexed briefly and allowed to stand at room temperature for 1 h, after which 6 μL of dye-labeled anti-phosphotyrosine was added to reach a final antibody/QD655 ratio of 16:1. The mixture was incubated for an additional 1 h at room temperature, protected from light, prior to recording photoluminescence spectra. Spectra in the range 490−730 nm (1 nm resolution) were measured on a SpectraMax M5 fluorescence microplate reader.

Control Samples. The four peptides used for the control samples were the following (see also Scheme 1): (A) AuNP-labeled uPA substrate peptide (biotin-SGRSANC-$CONH_2$); (B) uPA substrate peptide; (C) Her2 substrate peptide (HHHHHHGGGDNEYFYV-$CONH_2$); (D) Her2 control peptide (HHHHHHGGGDNE(pY)FYV-$CONH_2$). The QD525 controls (peptide A or B) were mixed with the QD655 controls (peptide C or D), giving rise to four possible permutations. The peptides were added to solutions of QD525 and QD655 at a 100:1 peptide/QD ratio. The mixture was vortexed briefly and allowed to stand at room temperature for 1 h, after which 6 μL of dye-labeled anti-phosphotyrosine was added to reach a final antibody/QD655 ratio of 16:1. The mixture was incubated for an additional 1 h at room temperature, protected from light, prior to recording photoluminescence spectra, as described above.

Acknowledgment. M.M.S. thanks the EPSRC for funding of S.B.L. Work at the Molecular Foundry was supported by the Director, Office of Science, Office of Basic Energy Sciences, Division of Materials Sciences and Engineering, of the U.S. Department of Energy under Contract No. DE-AC02-05CH11231.

Supporting Information Available: Supporting Figures S1−3. Calculation of limits of detection. Calculation of Förster radius. This material is available free of charge *via* the Internet at http://pubs.acs.org.

REFERENCES AND NOTES

1. Minelli, C.; Lowe, S. B.; Stevens, M. M. Engineering Nanocomposite Materials for Cancer Therapy. *Small* **2010**, *6*, 2336–2357.
2. Sapsford, K. E.; Pons, T.; Medintz, I. L.; Mattoussi, H. Biosensing with Luminescent Semiconductor Quantum Dots. *Sensors* **2006**, *6*, 925–953.
3. Pellegrino, T.; Kudera, S.; Liedl, T.; Javier, A. M.; Manna, L.; Parak, W. J. On the Development of Colloidal Nanoparticles towards Multifunctional Structures and Their Possible Use for Biological Applications. *Small* **2005**, *1*, 48–63.
4. Mart, R. J.; Osborne, R. D.; Stevens, M. M.; Ulijn, R. V. Peptide-Based Stimuli-Responsive Biomaterials. *Soft Matter* **2006**, *2*, 822–835.
5. Katz, E.; Willner, I. Integrated Nanoparticle-Biomolecule Hybrid Systems: Synthesis, Properties, and Applications. *Angew. Chem., Int. Ed.* **2004**, *43*, 6042–6108.
6. Ghadiali, J. E.; Lowe, S. B.; Stevens, M. M. Quantum-Dot-Based FRET Detection of Histone Acetyltransferase Activity. *Angew. Chem., Int. Ed.* **2011**, *50*, 3417–3420.
7. Laromaine, A.; Koh, L. L.; Murugesan, M.; Ulijn, R. V.; Stevens, M. M. Protease-Triggered Dispersion of Nanoparticle Assemblies. *J. Am. Chem. Soc.* **2007**, *129*, 4156–4157.
8. Harris, L.; Fritsche, H.; Mennel, R.; Norton, L.; Ravdin, P.; Taube, S.; Somerfield, M. R.; Hayes, D. F.; Bast, R. C. American Society of Clinical Oncology 2007 Update of Recommendations for the Use of Tumor Markers in Breast Cancer. *J. Clin. Oncol.* **2007**, *25*, 5287–5312.
9. Dano, K.; Andreasen, P. A.; Grondahlhansen, J.; Kristensen, P.; Nielsen, L. S.; Skriver, L. Plasminogen Activators, Tissue Degradation, and Cancer. *Adv. Cancer. Res.* **1985**, *44*, 139–266.
10. Schmitt, M.; Harbeck, N.; Thomssen, C.; Wilhelm, O.; Magdolen, V.; Reuning, U.; Ulm, K.; Hofler, H.; Janicke, F.; Graeff, H. Clinical Impact of the Plasminogen Activation System in Tumor Invasion and Metastasis: Prognostic Relevance and Target for Therapy. *Thromb. Haemostasis* **1997**, *78*, 285–296.
11. Slamon, D. J.; Clark, G. M.; Wong, S. G.; Levin, W. J.; Ullrich, A.; McGuire, W. L. Human Breast Cancer: Correlation of Relapse and Survival with Amplification of the HER-2/neu Oncogene. *Science* **1987**, *235*, 177–182.
12. Andrulis, I. L.; Bull, S. B.; Blackstein, M. E.; Sutherland, D.; Mak, C.; Sidlofsky, S.; Pritzker, K. P. H; Hartwick, R. W.; Hanna, W.; Lickley, L. neu/erbB-2 Amplification Identifies a Poor-Prognosis Group of Women with Node-Negative Breast Cancer. *J. Clin. Oncol.* **1998**, *16*, 1340–1349.
13. Xu, F. J.; Stack, S.; Boyer, C.; Obriant, K.; Whitaker, R.; Mills, G. B.; Yu, Y. H.; Bast, R. C. Heregulin and Agonistic Anti-p185(c-erbB2) Antibodies Inhibit Proliferation but Increase Invasiveness of Breast Cancer Cells that Overexpress p185(c-erbB2): Increased Invasiveness May Contribute to Poor Prognosis. *Clin. Cancer Res.* **1997**, *3*, 1629–1634.
14. Ignatoski, K. M. W.; Maehama, T.; Markwart, S. M.; Dixon, J. E.; Livant, D. L.; Ethier, S. P. ERBB-2 Overexpression Confers PI 3′ Kinase-Dependent Invasion Capacity on Human Mammary Epithelial Cells. *Br. J. Cancer* **2000**, *82*, 666–674.
15. Allgayer, H.; Babic, R.; Gruetzner, K. U.; Tarabichi, A.; Schildberg, F. W.; Heiss, M. M. c-erbB-2 Is of Independent Prognostic Relevance in Gastric Cancer and Is Associated with the Expression of Tumor-Associated Protease Systems. *J. Clin. Oncol.* **2000**, *18*, 2201–2209.
16. Konecny, G.; Untch, M.; Arboleda, J.; Wilson, C.; Kahlert, S.; Boettcher, B.; Felber, M.; Beryt, M.; Lude, S.; Hepp, H. HER-2/neu and Urokinase-Type Plasminogen Activator and its Inhibitor in Breast Cancer. *Clin. Cancer. Res.* **2001**, *7*, 2448–2457.
17. This calculation takes into account the wet biopsy weight of 500 mg, pulverized biopsy resuspension volume of 2 mL, and assumes 15% total protein per cell.
18. Goldman, E. R.; Clapp, A. R.; Anderson, G. P.; Uyeda, H. T.; Mauro, J. M.; Medintz, I. L.; Mattoussi, H. Multiplexed Toxin Analysis Using Four Colors of Quantum Dot Fluororeagents. *Anal. Chem.* **2004**, *76*, 684–688.
19. Medintz, I. L.; Clapp, A. R.; Brunel, F. M.; Tiefenbrunn, T.; Uyeda, H. T.; Chang, E. L.; Deschamps, J. R.; Dawson, P. E.; Mattoussi, H. Proteolytic Activity Monitored by Fluorescence Resonance Energy Transfer through Quantum-Dot-Peptide Conjugates. *Nat. Mater.* **2006**, *5*, 581–589.
20. Shi, L. F.; De Paoli, V.; Rosenzweig, N.; Rosenzweig, Z. Synthesis and Application of Quantum Dots FRET-Based

Protease Sensors. *J. Am. Chem. Soc.* **2006**, *128*, 10378–10379.
21. Kim, Y. P.; Oh, Y. H.; Oh, E.; Ko, S.; Han, M. K.; Kim, H. S. Energy Transfer-Based Multiplexed Assay of Proteases by Using Gold Nanoparticle and Quantum Dot Conjugates on a Surface. *Anal. Chem.* **2008**, *80*, 4634–4641.
22. Chang, E.; Miller, J. S.; Sun, J. T.; Yu, W. W.; Colvin, V. L.; Drezek, R.; West, J. L. Protease-Activated Quantum Dot Probes. *Biochem. Biophys. Res. Commun.* **2005**, *334*, 1317–1321.
23. Ghadiali, J. E.; Cohen, B. E.; Stevens, M. M. Protein Kinase-Actuated Resonance Energy Transfer in Quantum Dot-Peptide Conjugates. *ACS Nano* **2010**, *4*, 4915–4919.
24. Freeman, R.; Finder, T.; Gill, R.; Willner, I. Probing Protein Kinase (CK2) and Alkaline Phosphatase with CdSe/ZnS Quantum Dots. *Nano Lett.* **2010**, *10*, 2192–2196.
25. Han, M. Y.; Gao, X. H.; Su, J. Z.; Nie, S. Quantum-Dot-Tagged Microbeads for Multiplexed Optical Coding of Biomolecules. *Nat. Biotechnol.* **2001**, *19*, 631–635.
26. Ke, S.-H.; Coombs, G. S.; Tachias, K.; Corey, D. R.; Madison, E. L. Optimal Subsite Occupancy and Design of a Selective Inhibitor of Urokinase. *J. Biol. Chem.* **1997**, *272*, 20456–20462.
27. Kerman, K.; Song, H.; Duncan, J. S.; Litchfield, D. W.; Kraatz, H.-B. Peptide Biosensors for the Electrochemical Measurement of Protein Kinase Activity. *Anal. Chem.* **2008**, *80*, 9395–9401.
28. Xia, Z. Y.; Xing, Y.; So, M. K.; Koh, A. L.; Sinclair, R.; Rao, J. H. Multiplex Detection of Protease Activity with Quantum Dot Nanosensors Prepared by Intein-Mediated Specific Bioconjugation. *Anal. Chem.* **2008**, *80*, 8649–8655.
29. Sapsford, K. E.; Pons, T.; Medintz, I. L.; Higashiya, S.; Brunel, F. M.; Dawson, P. E.; Mattoussi, H. Kinetics of Metal-Affinity Driven Self-Assembly between Proteins or Peptides and CdSe/ZnS Quantum Dots. *J. Phys. Chem. C* **2007**, *111*, 11528–11538.
30. Pons, T.; Medintz, I. L.; Sapsford, K. E.; Higashiya, S.; Grimes, A. F.; English, D. S.; Mattoussi, H. On the Quenching of Semiconductor Quantum Dot Photoluminescence by Proximal Gold Nanoparticles. *Nano Lett.* **2007**, *7*, 3157–3164.
31. Nikiforov, T. T.; Beechem, J. M. Development of Homogeneous Binding Assays Based on Fluorescence Resonance Energy Transfer between Quantum Dots and Alexa Fluor Fluorophores. *Anal. Biochem.* **2006**, *357*, 68–76.
32. Prasuhn, D. E.; Deschamps, J. R.; Susumu, K.; Stewart, M. H.; Boeneman, K.; Blanco-Canosa, J. B.; Dawson, P. E.; Medintz, I. L. Polyvalent Display and Packing of Peptides and Proteins on Semiconductor Quantum Dots: Predicted Versus Experimental Results. *Small* **2010**, *6*, 555–564.
33. Dennis, A. M.; Sotto, D. C.; Mei, B. C.; Medintz, I. L.; Mattoussi, H.; Bao, G. Surface Ligand Effects on Metal-Affinity Coordination to Quantum Dots: Implications for Nanoprobe Self-Assembly. *Bioconjugate Chem.* **2010**, *21*, 1160–1170.
34. Jaiswal, J. K.; Goldman, E. R.; Mattoussi, H.; Simon, S. M. Use of Quantum Dots for Live Cell Imaging. *Nat. Methods* **2004**, *1*, 73–78.
35. Wang, J.; Xia, J. Preferential Binding of a Novel Polyhistidine Peptide Dendrimer Ligand on Quantum Dots Probed by Capillary Electrophoresis. **2011**, *83*, 6323−6329.
36. Pong, B. K.; Trout, B. L.; Lee, J. Y. Modified Ligand-Exchange for Efficient Solubilization of CdSe/ZnS Quantum Dots in Water: A Procedure Guided by Computational Studies. *Langmuir* **2008**, *24*, 5270–5276.